Electronic Supplementary Material (ESI) for Chemical Communications.
This journal is © The Royal Society of Chemistry 2021

Electronic Supplementary Information

Photothermal plasmonic microballs for a non-contact single-cell calcium ionophore delivery in heterogeneous cells

Vuong Thi Thanh Xuan Ho,[†a] Min Seok Song,[†a] Gun Kim,[†b] Nguyen Binh Nguyen,[a] Thi Phuong Dao,[a] So Yeong Lee,*[b] Sang-Woo Joo*

[a] Department of Information Communication, Materials, and Chemistry Convergence Technology, Soongsil University, Seoul 06978, Republic of Korea. Email: sjoo@ssu.ac.kr

[b] Laboratory of Veterinary Pharmacology, College of Veterinary Medicine and Research Institute of Veterinary Science, Seoul National University, 1, Gwanak-ro, Gwanak-gu, Seoul, Republic of Korea. Email: leeso@snu.ac.kr

[†] These authors contributed equally to this work.

Experimental Section

Materials

L-Ascorbic acid (≥ 99%), tetrachloroauric(III) acid trihydrate ($HAuCl_4.3H_2O$, ≥ 99%), thiol-PEG-amine (HS-PEG-NH_2, Mw ≈ 2000 g mol^{-1}, ≥ 99%), hexadecyltrimethylammonium bromide (CTAB, ≥ 99%), and silver nitrate ($AgNO_3$, ≥ 99%) were obtained from Sigma-Aldrich (St. Louis, USA). Sodium borohydride ($NaBH_4$, > 95%) and sodium hydroxide (NaOH, ≥ 98%) were obtained from Tokyo Chemical Industry (Tokyo, Japan). All chemicals were used without undergoing further treatment. The deionized water was purified using a Millipore Direct-Q 5 system with a resistivity of 18.0 megaohm cm.

Instrumental Measurements

HADDF-STEM measurements of AuNRs were conducted by a Cs-corrected JEOL JEM-ARM 200F electron microscope (Tokyo, Japan). The laser power and temperature values were obtained by an Ophir power meter (Darmstadt, Germany) and a FLIR C2 thermal camera (Wilsonville, USA). The microballs were characterized using a Zeiss Sigma VP FE-SEM microscope (Oberkochen, Germany). The UV-Vis-NIR absorption spectra were obtained by a Shimadzu 3600 plus spectrometer (Kyoto, Japan). The Raman signals were examined by a Renishaw confocal Raman system model Reflex microscope spectrometer at the excitation wavelength of 633 nm (Gloucesters, UK). LC-MS/MS measurements were obtained using a UHPLC System of Nexera X3 with the column of shim-pack GIST C18 (2.1 x 100 mm, 2 μm) and a Shimdazu LCMS-8060 spectrometer.

Microball Preparation

The glass surfaces were washed by ethanol solution (95%) and then pulled by PC-100 puller Narishige (Tokyo, Japan) in one step mode. A 0.25 mM solution of $HAuCl_4$ was prepared and adjusted pH to 12 by NaOH solution (1 M) and then mix well. Following, glass nanopipettes were backfilled with AA solution (0.1 M) by a microhose and subsequently immersed in prepared $HAuCl_4$ solution for 1 h at room temperature to form the gold microball.

Assembly of AuNRs on Microballs

The Au seeds were synthesized according to the literature [8b]. A solution including 10 mL of CTAB (0.1 M) and $HAuCl_4$ (0.25 mM) was vigorously stirred before the addition of 100 μL ice-cold $NaBH_4$ (0.06 M). The solution was then left stirred for 2 h at room temperature before further application. The ascorbic acid (190 μL, 0.03 M) was added to the mixture containing CTAB (10 mL, 0.1 M), $HAuCl_4$ (100 μL, 0.05 M), and $AgNO_3$ (155 μL, 3 mM). When the color became colorless, 12 μL of seed solution was added to the growth solution under gentle stir. After 2 h, The products were centrifuged for 5 min at 5000 rpm to remove excess CTAB and re-dispersed in 10 mL of H_2O for further modification. The CTAB ligands on the surface of AuNRs were removed by NH_2-PEG-SH. 1 ml of NH_2-PEG-SH (3 mM) was added dropwise to AuNRs solution under vigorously stirring and then was left stirring for 24 h. The solution was washed twice times by centrifugation (5000 rpm, 5 min) and was finally dispersed in 5 mL of water. 10 mL of AuNRs/NH_2-PEG-SH were centrifuged at 5000 rpm for 5 min to remove excess CTAB and NH_2-PEG-SH and then re-dispersed in 5 mL of water. Subsequently, the microballs on the tip of nanopipettes were immersed into the AuNRs/NH_2-PEG-SH solution, following stirring 2 h in room temperature and gold microballs coated with AuNRs were formed. Resulting products were washed by pure water and dried at room temperature. A gold microball was directly synthesized on the tip of the nanopipettes by reduction reaction between ascorbic acid (AA) and chloroauric acid ($HAuCl_4$). AuNRs–NH_2 was dispersed in 5 mL of water and then the nanopipette-gold spheres were immersed into AuNRs solution, following stirring in 2 h in room temperature and gold ball coated AuNRs were formed. As for milliballs, a 1.0 mm-diameter glass bead

was attached to a borosilicated-glass capillary micropipette by alcohol lamp fire. The glass balls were first immersed in 10% NaOH solution under gentle stirring for 1 h to ionize the glass surfaces. Subsequently, the activated balls were covered by GPTMS (4.5%, v/v) in pure ethanol (≥ 99.9%) at 45 °C for 12 h, followed by thoroughly rinsing with ethanol under mild sonication and drying at ambient conditions. The microball surfaces covered with GPTMS groups were reacted with the NH_2-PEG-SH-coated AuNRs by immersing the pipette into the AuNRs solution under light stirring at 45 °C.

Assembly of AuNRs on glass surface

Due to the too small surface of the microball (gold sphere@AuNRs), it was impossible to observe the temperature increasing phenomena using FLIR camera. Thus, we mimicked the surface of microball fully covered by AuNRs by using the AuNR-modified glass surface (Fig. S4). First, we soaked a piece of glass (4 mm x 30 mm) in NaOH 1M solution for 2h to obtain the negative charge surface. Then the glass was rinsed carefully with distilled water before being put in a vial containing 3 mL of NH_2-PEG-SH-coated AuNRs without stirring for 2h. The attaching surface of the glass with NH_2-PEG-SH-coated AuNRs was resulted from electrostatic interaction between the different charge surfaces. Thermal imaging on the surface of glasses was investigated using a FLIR camera C2 (Wilsonville, USA), object temperature ranging from −10°C to 150°C.

Cell Culture and Fluorescence Observation

Four different human cancer cell lines were used for in vitro experiments: A431, HeLa, MDA-MB-453, and MDA-MB-453 CSC. RPMI 1640 (for A431) and DMEM (for HeLa, MDA-MB-453 and MDA-MB-453 CSC) were used as cell culture media, supplemented with 1% penicillin and 10% FBS solution. The cells-containing petri dish was incubated overnight at 37 °C, 5% CO_2 atmosphere incubator until confluence of grown cells got approximately 80%. The old cell medium then was removed and washed with DBPS. Cells from the bottom of the dish were detached by trypsin and centrifuged at 1200 rpm for 3 min to discard trypsin and media. Cells were re-suspended in the confocal dish, which previously contained 2 mL of media and maintained consistently at 37 oC, 5% CO_2 atmosphere incubator to prepare for fluorescence experiments. HeLa (KCLB #10002) and A431 (KCLB #21555) cell lines were obtained from Korean Cell Line Bank (Seoul, Korea). MDA-MB-453 and MDA-MB-453 CSC were kindly provided by Dr. Kwon at Seoul National University. MDA-MB-453 CSC has been shown to have cancer stem cell-like properties compared to its parental cell line.[S1] For Ca^{2+} signal, cells were incubated with Fluor 4-AM at 0.5% for 30 min, washed by DPBS and changed to normal cell medium. Hoechst 33342 was likewise stained at 0.05% for 5 min, washed by DPBS. Annexin V was stained at 0.5% and the cells were observed up to 3 h.

Interactions of Microball Tips on a Single Cell Investigated by Raman Spectroscopy

Microball tips were engaged and penetrated to the cells by Raman spectroscopy. Surface-enhanced Raman spectroscopy (SERS) was introduced to check the physical parameters for the release of the adsorbates coated on a microball tip. The drug compound was heated up by the temperature generated from the laser spot leading to a thermal desorption. A laser power-dependent experiment was tested at the ambient condition using a 633 nm laser whose wavelength matched the transverse mode of the synthesized AuNRs with intensity from 2 μW to 75 μW to observe the thermal decomposition. An AuNR-coated microball tip was immersed in mitoxantrone (MTX) 10^{-4} M solution in 2 h to load on the AuNR surface, and then washed by distilled water to be submitted directly to SERS measurement. The pipette was approximately tilted at an angle of 30° degrees from horizontal plane. The microball was slowly moved down to approach the cell vertically. When the microball reached the cell nucleoplasm (determined by the microscopic focus and the morphological change of the cell), the laser was irradiated at the microball. Fig. S9 shows the decrease in the intensities of 1295 cm^{-1} peak which represent the release of MTX under 0–300 s laser irradiation. It was shown that 45% of MTX was released rapidly from the AuNRs-microball surface within the initial 30 s of irradiation, and the release rate was slower in the following 270 s. After 300 s, 85% of

MTX was released from the microball. The cell images were obtained using an Olympus IX-71 inverted microscope integrated with a Coolsnap HQ CCD camera and a 10X objective lens. All images were captured and analyzed by MetaMorph software.

COMSOL Modeling and Calculations

COMSOL Multiphysics 5.6 were employed for drug diffusion simulation. Using the geometry tools provided by COMSOL, the adherent cells, the microball and the pipette, and the confocal dish were constructed. The distance between the target and the adjacent cells was set as 35 μm, which is an average of the intercellular distances measured by connecting the centers of the HeLa cells on the confocal microscopy image. The radius of the microball was 1.25 μm, attached to a glass pipette at an angle of 30°. The glass pipette tip angle was measured to be 5°, as reflected in the geometry. The position of the microball was measured by the micromanipulator and was set as 5 μm from the top of the cell. The chamber where the drug will be randomly diffused was constructed to be 17.15 mm in radius and 2.166 mm in height, which was calculated based on 2 mL cell medium in the confocal dish.
The cell surface was set as a thin diffusion barrier with the thickness[S2] of 4.25 nm and diffusion coefficient of 4.14×10^{-10} m^2 s^{-1}. The diffusion coefficient was determined by Stokes-Einstein equation as described by Leedale et al.[S3] Each parameter and condition was set as follows: temperature: 25℃; viscosity of medium: 8.90×10^{-4} kg m^{-1} s^{-1};[S4] A23187 molecular weight: 523.62 g mol^{-1}; density: assumed as 1 g cm^{-3}.
To compare the amounts of A23187 arriving the target cell and the adjacent cell, we designated one half of the microball surface to give an instantaneous (1 ms) flux of the drug, in an attempt to simulate the photothermal release from the surface where the laser is directly irradiated at the angle of 60°. The flux was set so that the total amount of release would match the expected average released amount of A23187 from microball (6.7194×10^{-19} mol; Fig. S7). From the calculated surface area of 8.5895×10^{-12} m^2 of the microball hemisphere, the flux was determined to be $(6.7194 \times 10^{-19}$ mol) / $(8.5895 \times 10^{-12}$ $m^2)$ / $(10^{-3}$ $s^{-1})$ = 7.8228×10^{-5} mol m^{-2} s^{-1}. The drug amount arriving the target or the adjacent cell surface was calculated according to COMSOL drug transport module.

DFT Calculations

Simulated Raman spectra and potential energy distribution (PED) calculations were performed similarly to a previous report.[S5] Using Gaussian 09 software we have calculated the quantum chemical density functional theory (DFT) calculations for Raman vibrational frequencies of A23187 on the gold surface (**Fig. S5**) using the RB3LYP/LANL2DZ method. Subsequently, Raman vibrational assignments of A23187 (**Table S1**) were obtained based on PED calculations and analyzed in detail with the vibrational energy distribution analysis (VEDA) program, which directly and automatically read the input data from the Gaussian program output files.

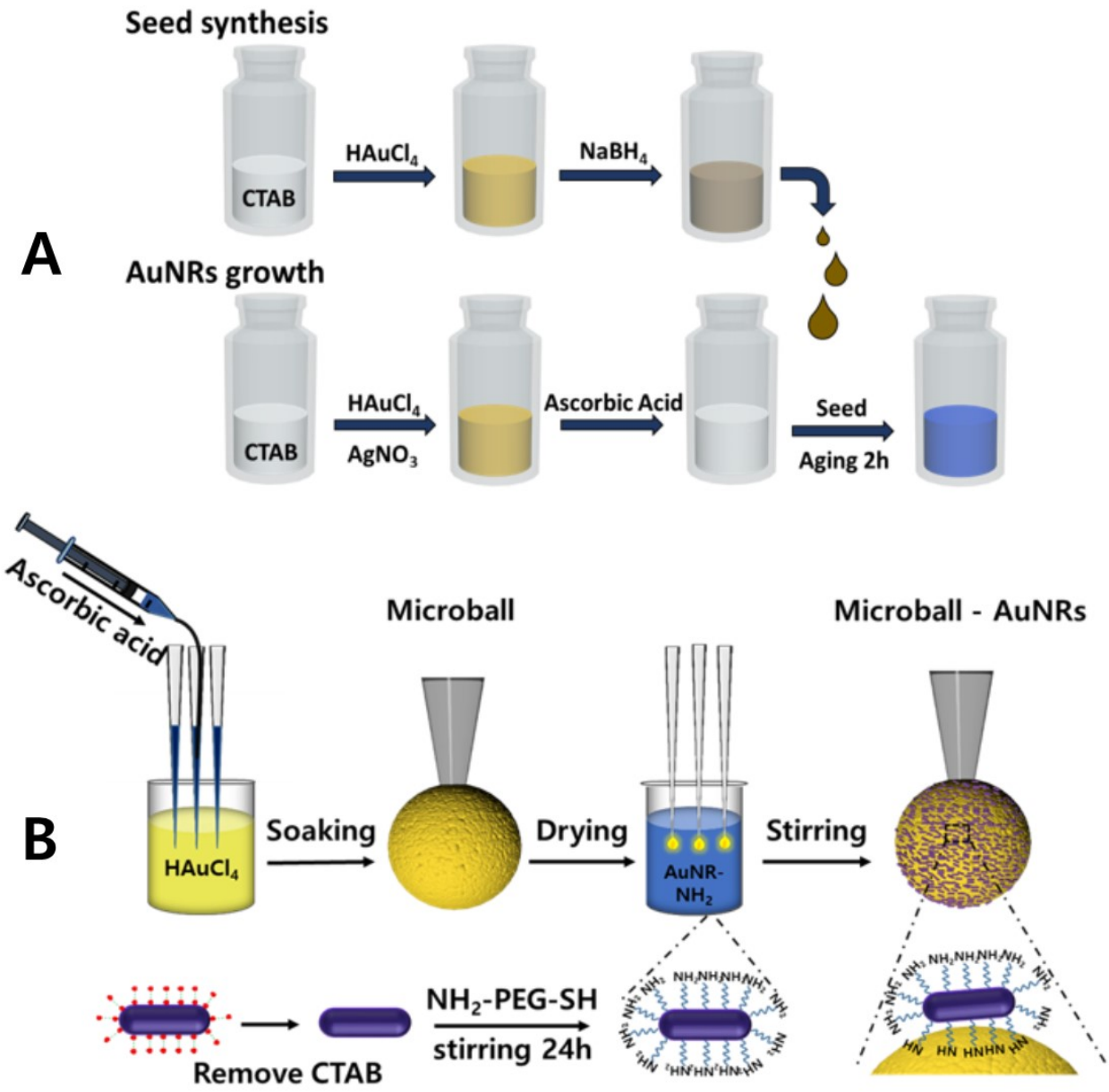

Fig. S1. Schematics of (a) AuNR synthesis and (B) fabricating microball decorated AuNRs on pipette tip.

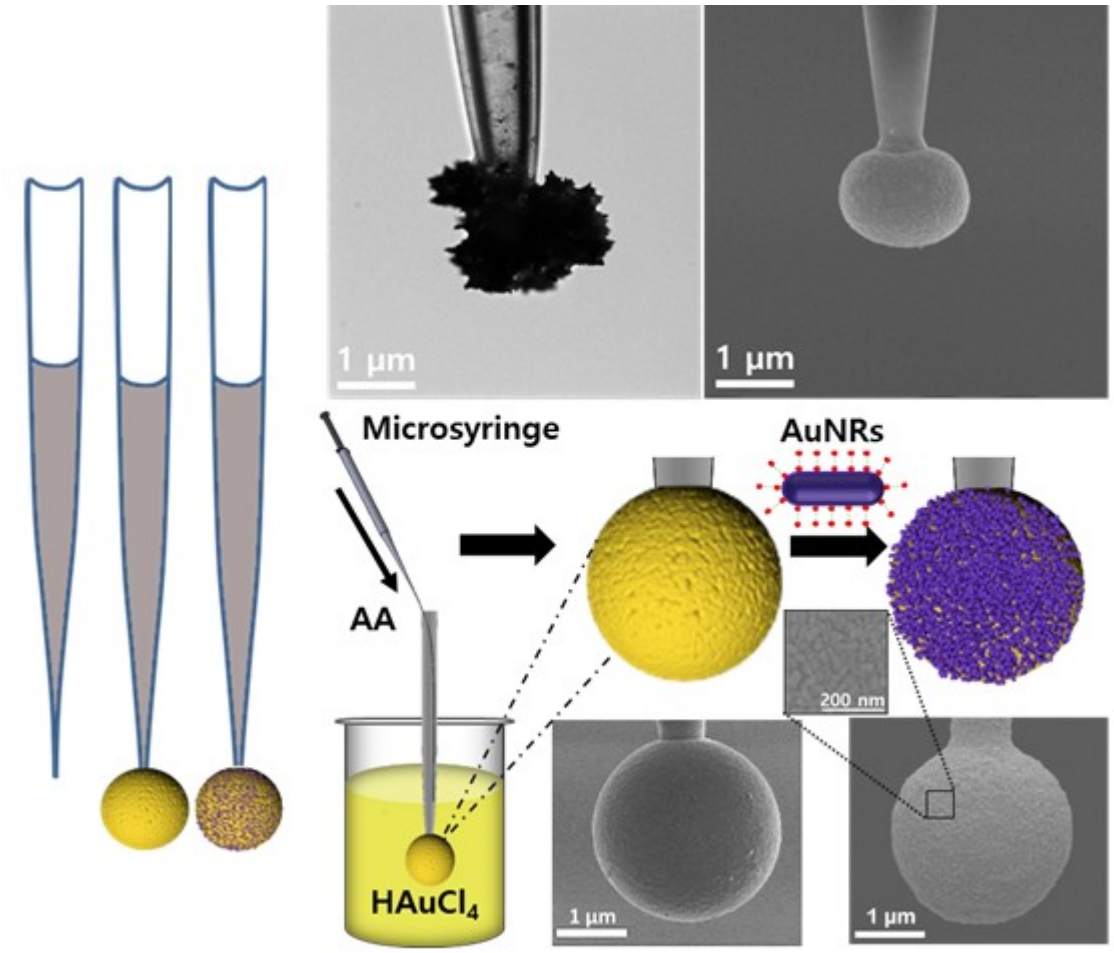

Fig. S2. A photothermal plasmonic AuNR microball attached to a glass micropipette via a microhose from 0.1 M AA in 0.25 mM $HAuCl_4$ at pH 12.

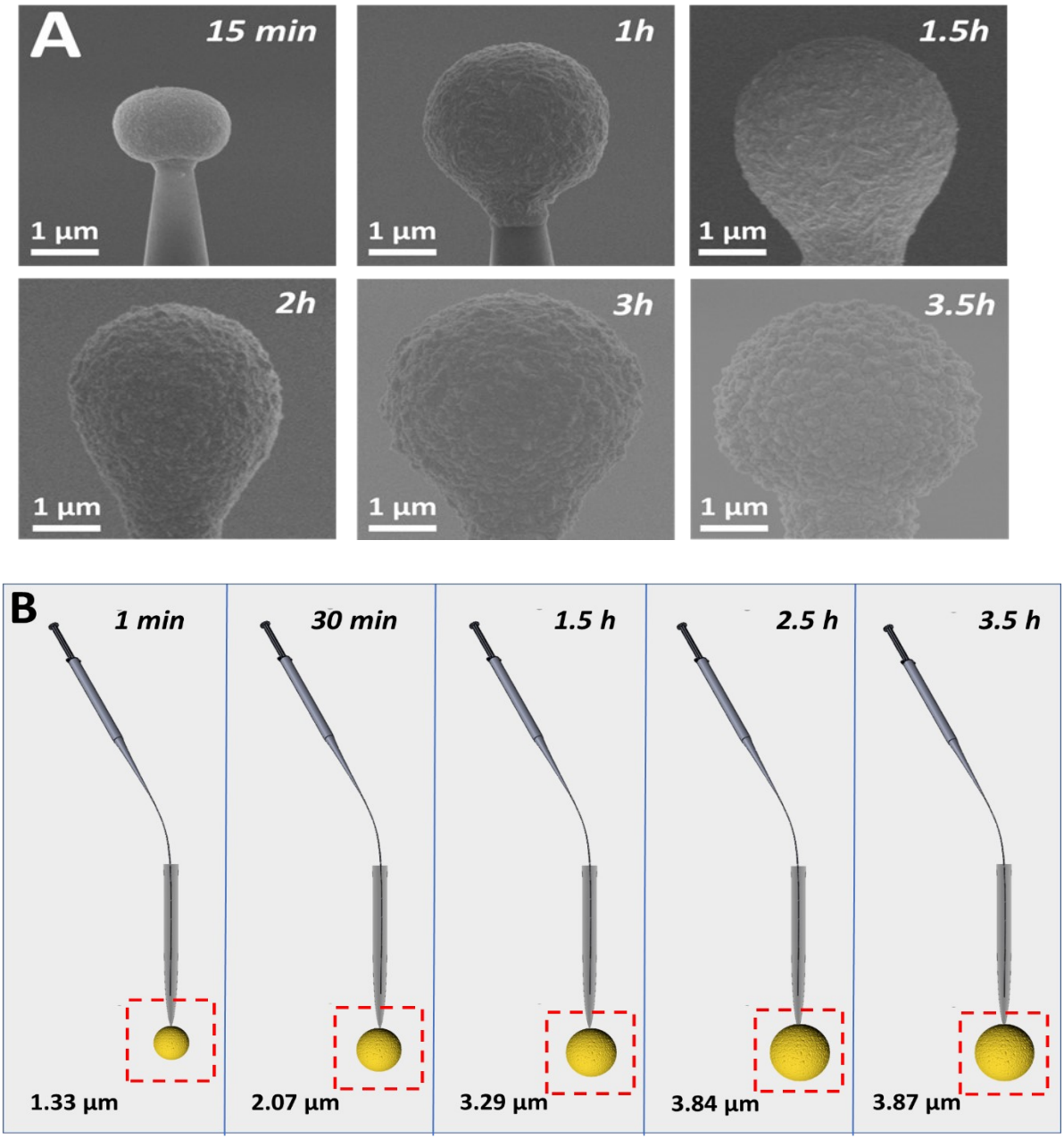

Fig. S3. (A) SEM images of the microballs according to the reaction time. (B) An illustrative depiction of (A). The parts are not drawn to their exact scales. The sizes of the gold microspheres were not consistent enough throughout the first 5 min of the reaction. They became consistent after 6 min of incubation. The gold sphere-pipette structures with sphere sizes between 0.7 µm – 1.5 µm were somewhat stable and were easily broken at the pipette tip.

Fig. S4. Photothermal temperature rises of AuNRs assembled on glass plates irradiated with 30 mW, 671 nm laser.

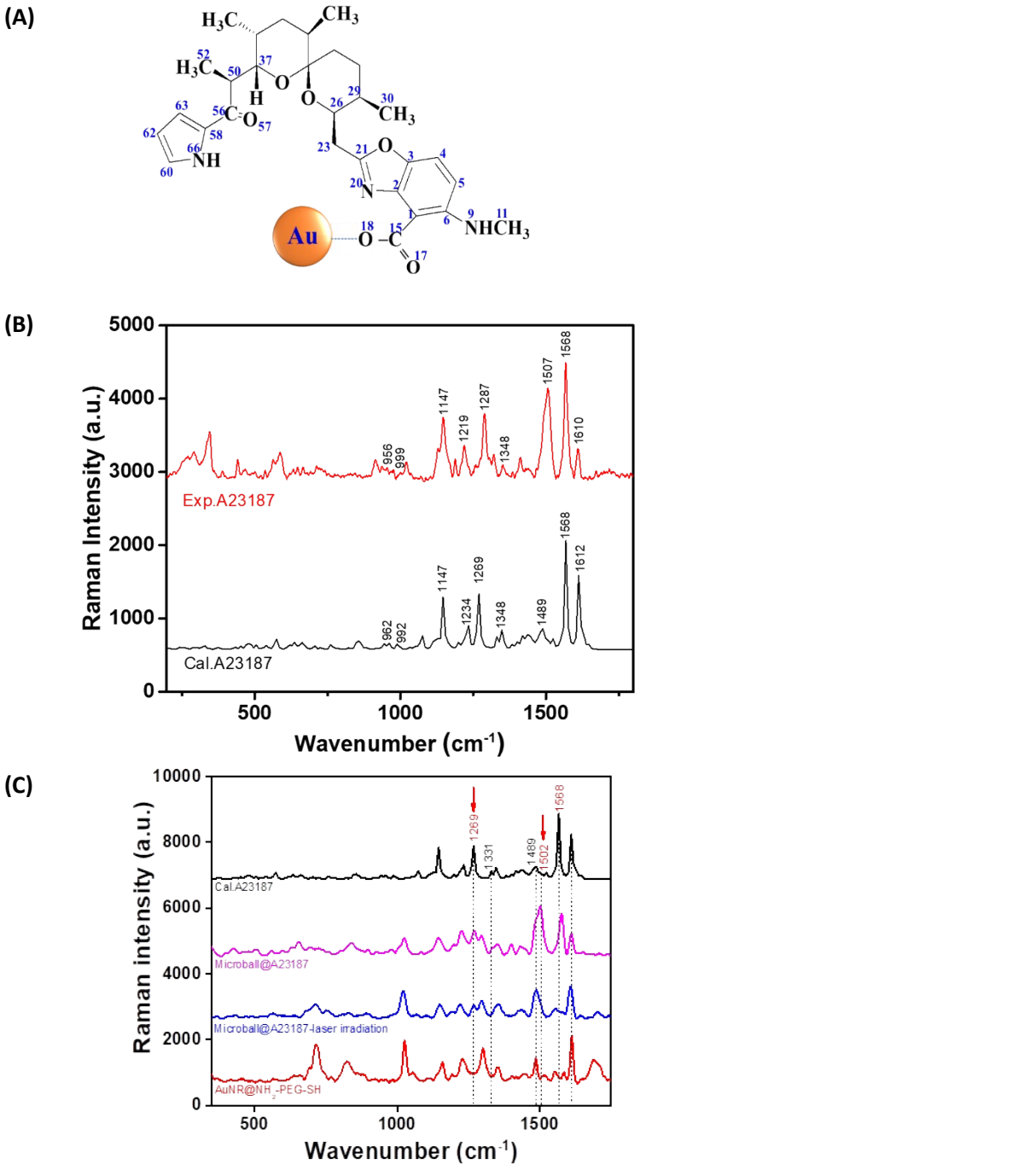

Fig. S5. (A) A23187 structure and its numbered structure. (B) Experimentally measured and theoretically calculated Raman vibrations of A23187. (C) Reduction of SERS intensity of A23187 after laser treatments. The calculated A23187 spectrum is shown (black). Before the laser treatment, the SERS spectrum of Microball@A23187 revealed strong signal at the bands of 1502 cm^{-1} and 1570 cm^{-1}, which is interpreted as the A23187 molecules on the surface of the microball (pink). After the laser irradiation, there was a significant decrease in the peaks at 1502 cm^{-1} and 1570 cm^{-1} (blue), and the overall spectrum became similar to the AuNR@NH2-PEG-SH spectrum (red).

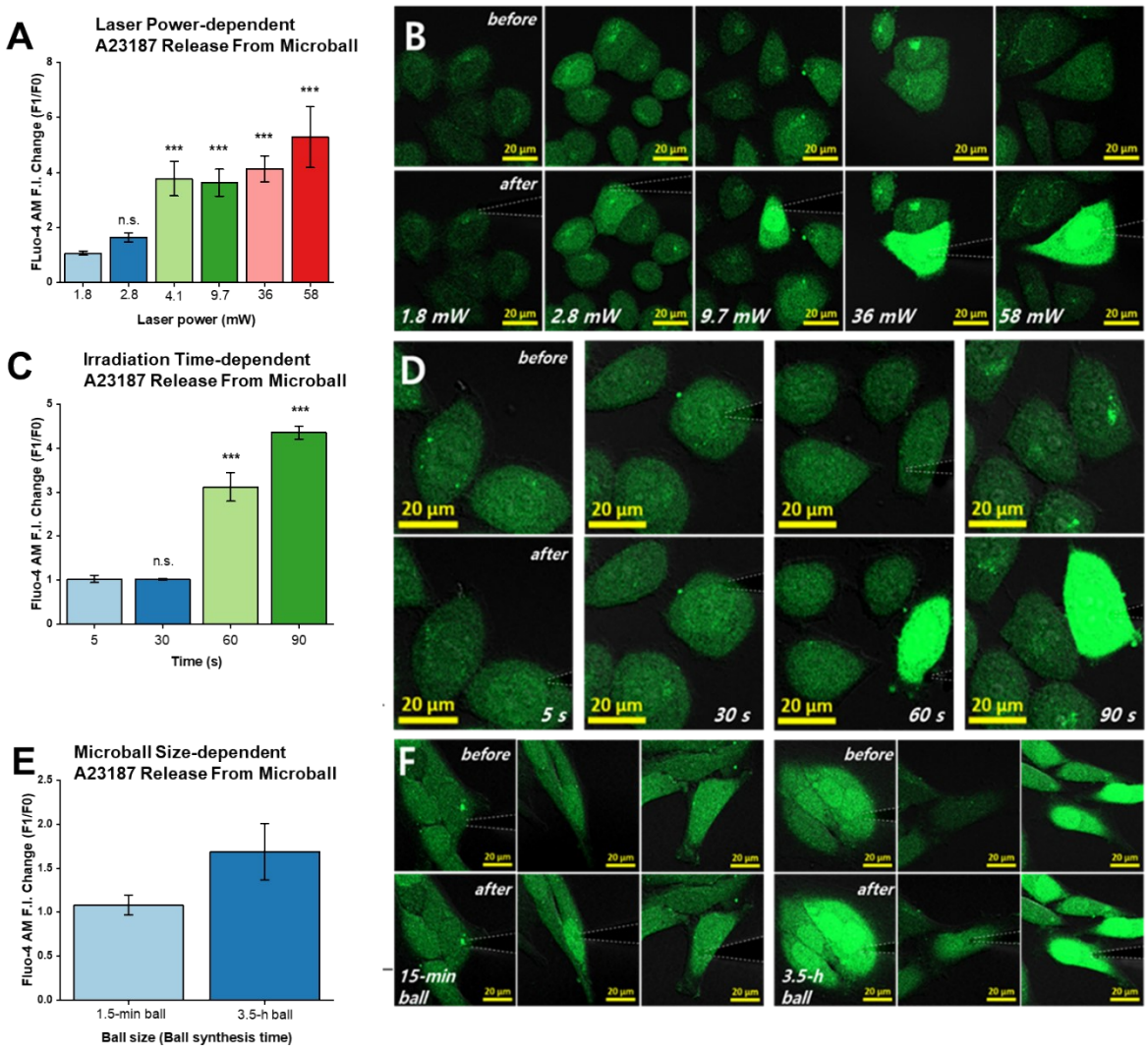

Fig. S6. (A) Laser power-dependent fluorescence changes (Irradiation time: 90 s) (B) Laser irradiation time-dependent fluorescence changes (Laser power: 9.7 mW). Statistical analysis for A and B was done with one-way ANOVA and Tukey's multiple comparison test (n = 5-9 and n = 2-5, respectively). (C) Microball size-dependent fluorescence changes (Irradiation time and laser power: 90 s and 9.7 mW, respectively; n = 3). (D) Representative images of laser power-dependent fluorescence changes (Irradiation time: 90 s). (E) Representative images of laser time-dependent fluorescence changes (Laser power: 9.7 mW). The laser beam diameter was 2 mm, which makes the laser powers in the experiment, in the increasing order, 57.3 mW/cm^2, 89.1 mW/cm^2, 308.8 mW/cm^2, 1145.9 mW/cm^2, and 1846.2 mW/cm^2, respectively. (F) Representative images of the microball size-dependent fluorescence changes.

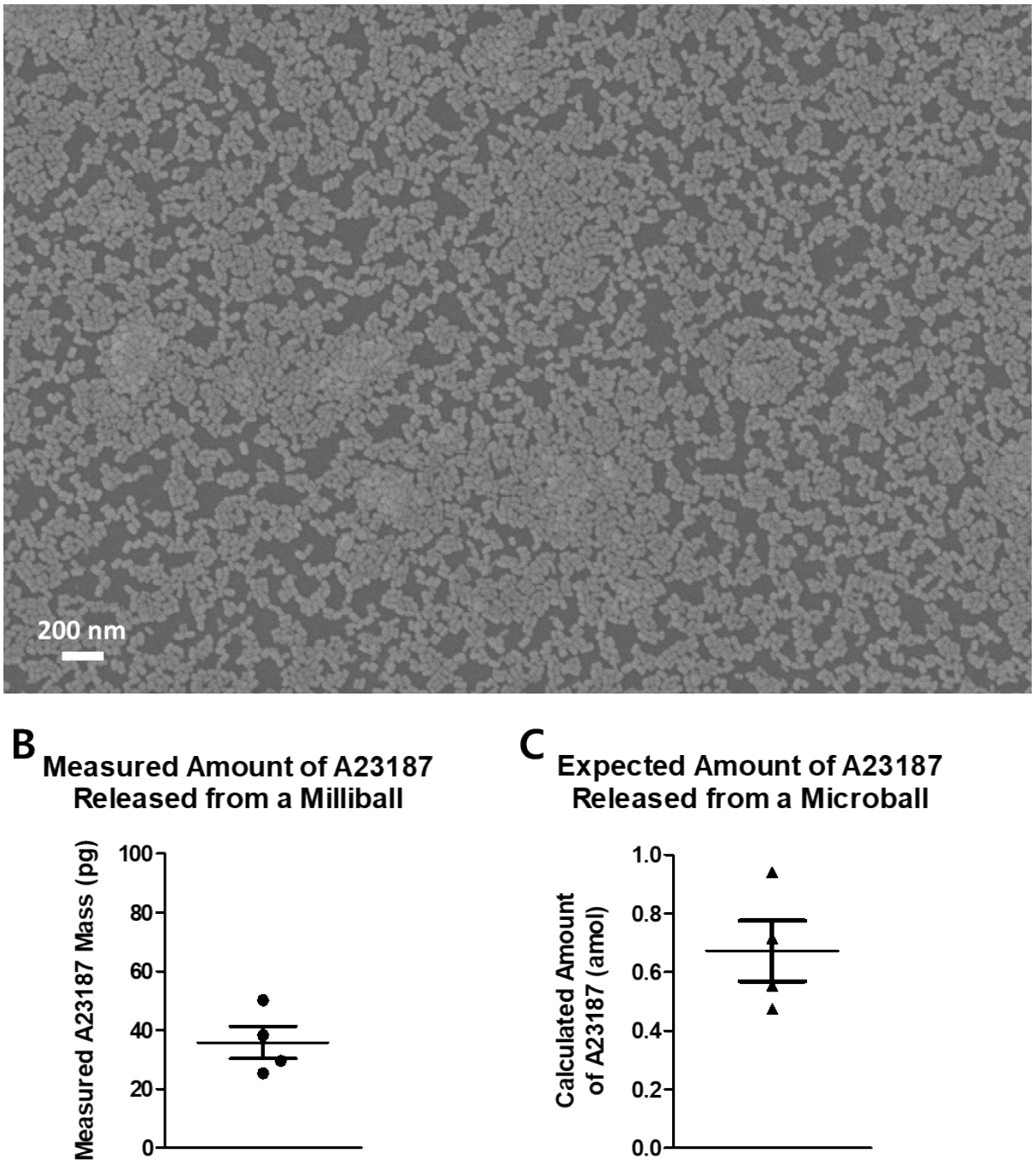

Fig. S7. (A) The AuNR coverage of milliball was estimated to be 63.7%. (B) The LC-MS/MS analysis suggests the amount of A23187 from a milliball to be 36 fg. (C) The A23187 amount from a microball is expected to be ~0.67 amol.

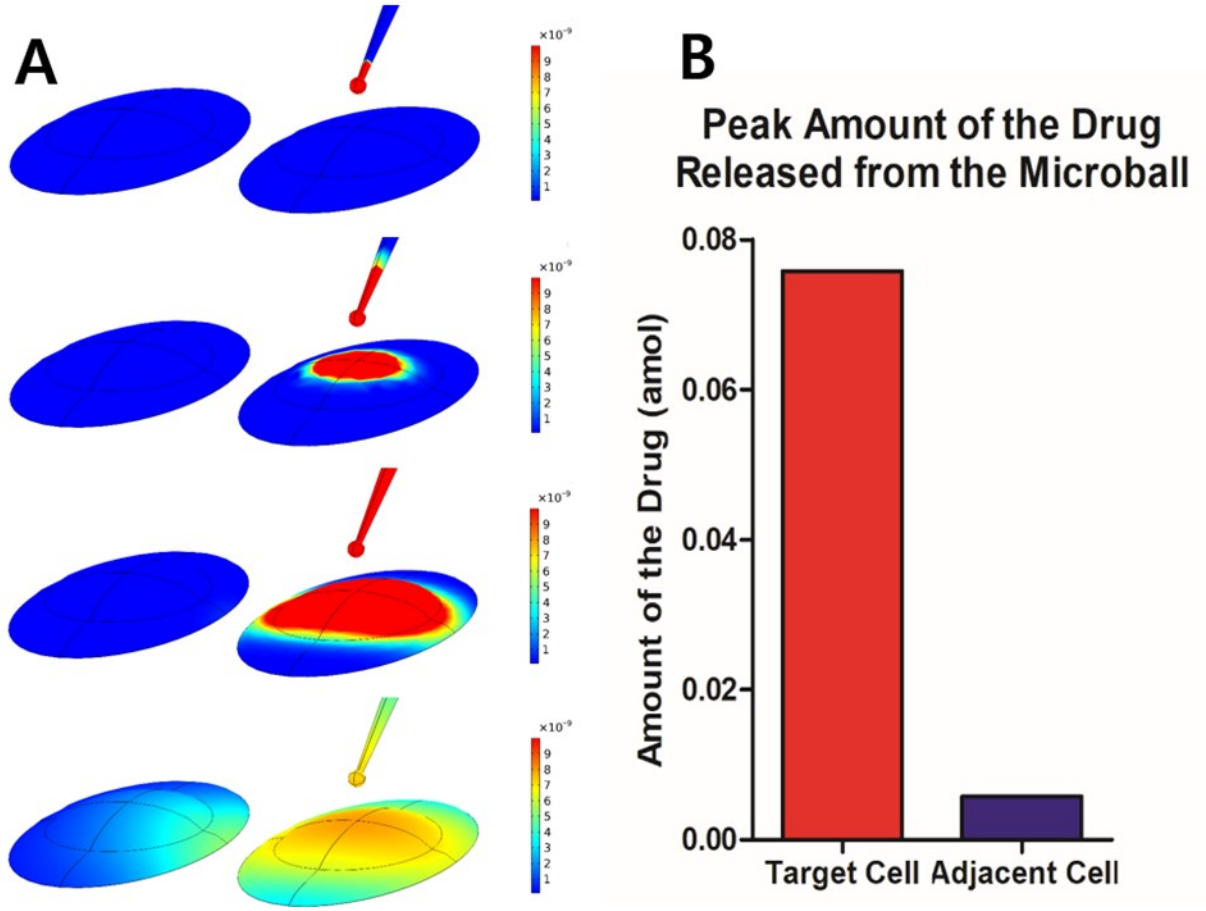

Fig. S8 (A) Visual time-lapse illustration of the drug released from the microball arriving at the target cell (right) surface compared to the adjacent cell (left) at 0.005. 0.01. 0.05, and 0.5 s. (B) Tested at different amounts of drug loads, the drug concentration in the target cell was estimated to be larger by 13.2 times than those in the adjacent cells.

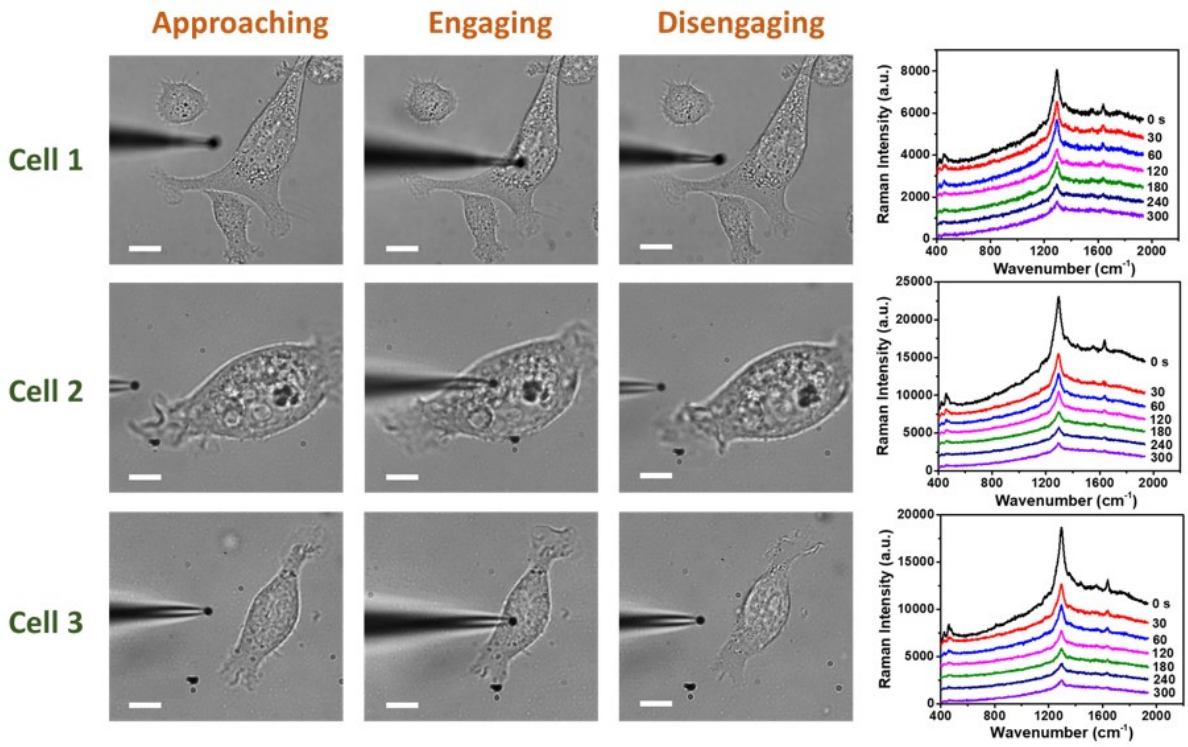

Fig. S9 Phase contrast images showing the microballs and time-dependent SERS spectra of MTX-conjugated AuNRs on a microball showing the release of MTX according to 633 nm laser irradiation.

References

Ref. S1 Y.D. Yoo, D.H. Han, J.M. Jang, A. Zakrzewska, S-Y. Kim, C. Y. Choi, Y. J. Lee and Y.T. Kwon, *Anticancer Res.,* 2013, **33**, 763–777.

Ref. S2 K. Mitra, I. Ubarretxena-Belandia, T. Taguchi, G. Warren, D. M. Engelman, *Proc. Natl. Acad. Sci. U. S. A.,* 2004, **101**, 4083–4088.

Ref. S3 J.A. Leedale, J.A. Kyffin, A.L. Harding, H.E. Colley, C. Murdoch, P. Sharma, D.P. Williams, S.D. Webb, R. N. Bearon, *Interface Focus,* 2020, **10**, 20190041.

Ref. S4 J. C. Crittenden, R. R. Trussell, D. W. Hand, K. J. Howe and G. Tchobanoglous, *MWH's Water Treat.*, 2012, Appendix C: Physical Properties of Water, 1861–1862.

Ref. S5 N. H. Ly, T. H. Nguyen, N. Đ. Nghi, Y. H. Kim and S. W. Joo, *Sensors*, 2019, **19**, 1355.

Table S1. Experimentally measured and theoretically calculated Raman vibrations of A23187, respectively.

SERS	DFT	Assignments
1610	1612	$\nu(C_4–C_3)$ (13%) + $\nu(C_3–C_2)$ (27%) + $\beta(C_2–C_1–C_6)$ (10%)
1568	1568	$\nu(N_{20}–C_{21})$ (54%) + $\nu(C_{23}–C_{21})$ (14%)
1507	1489	$\beta(H_{31}–C_{30}–H_{33})$ (52%) + $\beta(H_{32}–C_{30}–H_{31})$ (15%)
1348	1348	$\delta(H_{25}–C_{23}–C_{26}–C_{29})$ (13%) + $\delta(H_{24}–C_{23}–C_{26}–C_{29})$ (31%)
1287	1269	$\beta(H_{51}–C_{50}–C_{52})$ (46%) + $\delta(H_{53}–C_{52}–C_{50}–C_{37})$ (13%)
1219	1234	$\nu(C_3–C_2)$ (10%) + $\nu(C_{15}–C_1)$ (10%) + $\beta(H_{19}–O_{18}–C_{15})$ (16%)
1147	1147	$\beta(H_7–C_4–C_5)$ (14%) + $\delta(H_{13}–C_{11}–N_9–C_6)$ (10%)
999	992	$\nu(O_{22}–C_3)$ (22%) + $\nu(C_{15}–C_1)$ (20%)
956	962	$\nu(C_{62}–C_{63})$ (32%) + $\beta(C_{62}–C_{63}–N_{66})$ (10%) + $\beta(C_{63}–N_{66}–C_{58})$ (17%) + $\delta(H_{61}–C_{60}–C_{62}–C_{63})$ (11%)

Scale factor (0.9765) was applied. Abbreviations: δ; Torsion, ν; stretching, β; bending. Unit in cm^{-1}. Atomic numbering depicted in **Figure S5A**.